

## Article

# Optimization Study of Annular Wear-Resistant Layer Structure for Blast Furnace Tuyere

Wentao Zhu <sup>1</sup>, Jianliang Zhang <sup>1,2</sup>, Yanbing Zong <sup>1</sup>, Lei Zhang <sup>3,\*</sup>, Yanxiang Liu <sup>1</sup>, Lifeng Yan <sup>4</sup> and Kexin Jiao <sup>1,3</sup>

<sup>1</sup> School of Metallurgical and Ecological Engineering, University of Science and Technology Beijing, Beijing 100083, China; m202120353@xs.ustb.edu.cn (W.Z.); zhang.jianliang@hotmail.com (J.Z.); zongyb@ustb.edu.cn (Y.Z.); liuyanxiang@ustb.edu.cn (Y.L.); jiaokexin@ustb.edu.cn (K.J.)

<sup>2</sup> State Key Laboratory of Advanced Metallurgy, University of Science and Technology Beijing, Beijing 100083, China

<sup>3</sup> Research Institute of Macro-Safety Science, University of Science and Technology Beijing, Beijing 100083, China

<sup>4</sup> Wanfeng Metallurgical Spare Parts Co., Ltd., Zhangjiakou 076250, China; 15831389099@163.com

\* Correspondence: b2130760@ustb.edu.cn

**Abstract:** A new tuyere small sleeve coating structure that balances the high thermal conductivity of the copper substrate with the high wear resistance of the protective layer was developed in this paper. This structure can achieve a low-carbon blast furnace by reducing the heat loss from the tuyere. The 3D model was established via Solidworks for modeling and Ansys for numerical simulation, the temperature field of the annular wear-resistant layer structure tuyere small sleeve with different widths of the wear-resistant layer was analyzed and compared with the temperature and stress field of traditional tuyere small sleeve. The results show that the design of the annular wear-resistant layer structure of the tuyere small sleeve is more effective. The new annular wear-resistant layer structure for the tuyere small sleeve results in a decrease of 24 K in the average temperature of the wear-resistant coating. The comparison of this structure with tuyere sleeves without wear-resistant coatings shows a 16.7% reduction in heat loss, improves the wear resistance of the tuyere, providing new technological ideas for low-carbon blast furnace production. Compared with the tuyere sleeve completely covered with a wear-resistant coating, the maximum thermal stress of this structure decreased from 624.98 Mpa to 427.99 Mpa, resulting in a reduction of 31.5%, which is beneficial for the service life of the tuyere sleeve. The copper surface temperature of the new tuyere small sleeve is in a safe range when the temperature is below 2273 K.

**Keywords:** blast furnace tuyere; wear-resistant layer; temperature field; stress field; low-carbon technology



**Citation:** Zhu, W.; Zhang, J.; Zong, Y.; Zhang, L.; Liu, Y.; Yan, L.; Jiao, K. Optimization Study of Annular Wear-Resistant Layer Structure for Blast Furnace Tuyere. *Metals* **2023**, *13*, 1109. <https://doi.org/10.3390/met13061109>

Academic Editor: Yadir Torres Hernández

Received: 27 April 2023

Revised: 5 June 2023

Accepted: 9 June 2023

Published: 13 June 2023



**Copyright:** © 2023 by the authors. Licensee MDPI, Basel, Switzerland. This article is an open access article distributed under the terms and conditions of the Creative Commons Attribution (CC BY) license (<https://creativecommons.org/licenses/by/4.0/>).

## 1. Introduction

Advanced equipment is a prerequisite for safe and low-carbon development in the high-temperature metal smelting industry. The tuyere small sleeve is essential metallurgical equipment for blast furnace smelting, and the length of its lifespan directly affects the smooth operation and output of the blast furnace [1]. The tuyere small sleeve is located between the belly and waist of the blast furnace and is responsible for providing hot air and fuel, such as coal powder, to the furnace. Its working environment is extremely harsh. On one hand, the tuyere small sleeve end is repeatedly bonded and peeled off by the high-temperature slag and iron, causing the melting and erosion failure of the tuyere small sleeve end [2–4]. On the other hand, the hot air and fuel supplied by the tuyere small sleeve to the furnace undergo violent combustion under high-temperature and high-pressure conditions [5], leading to the tuyere small sleeve end bearing a huge thermal load. Tuyere small sleeve damage poses a serious safety hazard by causing water leakage in the blast furnace, and the replacement of the tuyere small sleeve leads to production disruption affecting the stable operation of the blast furnace. Currently, the lifespan of tuyere small

sleeves varies both domestically and internationally, with frequent damage to tuyere small sleeves of large blast furnaces, and the lifespan not meeting the design expectations [6].

In recent years, there have been two main approaches to optimize the tuyere small sleeve due to its tendency to easily become damaged [7,8]. One method is to enhance the tuyere small sleeve's heat dissipation capability at the front end by optimizing the water structure inside the tuyere. Rajeswar Chatterjee et al. [9–11] successfully extended the lifespan of the tuyere small sleeve by three months through numerical simulation to optimize the aspect ratio of the front-end cooling water pipeline, strengthening the front-end water velocity to reduce the occurrence of film boiling phenomenon. In addition, Guo X.P. et al. [12] investigated the impact of tuyere small sleeve structure on temperature and stress fields through numerical simulations. The results showed that optimizing the internal structure of the tuyere was beneficial for reducing both temperature and stress.

Another method is to apply surface treatment to the tuyere small sleeve and select coatings of different materials to enhance the wear resistance and anti-melting capacity of the tuyere small sleeve. Radyuk, A.G. et al. and Tarasov, Y.S. et al. [13–15] conducted numerical simulations using DEFORM-2D and Ansys to demonstrate the benefits of using refractory coatings on tuyeres. Their study showed that tuyeres with refractory coatings experience reduced thermal flux intensity and lower stress on the inner surface compared to tuyeres without wear-resistant coatings. This finding highlights the potential for extended tuyere lifespan. Zhang, J. et al. [16] proposed the application of wear-resistant coatings to protect the front end and inner wall of the tuyere, with the aim of extending its service life. Zhiyu Chen et al. [17] used CFD simulations to investigate the temperature field of the tuyere small sleeve with Ni60A coatings containing different copper contents. The results showed that the front-end temperature of the tuyere was directly related to the coating material. Li D et al. [18] prepared a dual-phase wear-resistant layer structure of Co66/Ni60A using plasma cladding technology, which established a gradient temperature field at the front end of the tuyere and is referred to as a gradient wear-resistant layer. This new coating structure has been shown to have better long-term stability during use.

Each of these two optimization methods has its own advantages and disadvantages. The method of optimizing the internal water structure can effectively enhance the front-end heat dissipation capability of the tuyere small sleeve, but due to the harsh environment inside the blast furnace, the surface of the tuyere small sleeve is prone to wear and corrosion, leading to limited optimization effects. On the other hand, the method of surface coating treatment can enhance the wear resistance and anti-melting capacity of the tuyere small sleeve [19,20], but the addition of the coating may affect the thermal conductivity of the tuyere small sleeve, causing it to lose some of its heat dissipation capacity and posing a safety hazard. Currently, further research is needed on how to enhance the wear resistance and anti-melting capacity of the tuyere small sleeve while ensuring its heat dissipation capability and safety.

This study focuses on the optimization of the coating structure for the current double-inlet and double-outlet tuyere small sleeve. The tuyere small sleeves on the market currently have safety issues of wear and melting, and coatings can effectively improve the tuyere small sleeve's wear resistance and anti-melting capacity. However, the coating to some extent reduces the high thermal conductivity of copper material. Therefore, we propose a new optimization solution, which is to add annular heat dissipation openings on the surface of the tuyere small sleeve coating. This can both utilize the high thermal conductivity of copper material and obtain the wear resistance and anti-melting capacity of the coating. In order to investigate the influence of different coating structures on the heat transfer performance of the tuyere small sleeve, we established finite element models of tuyere small sleeves with different coating structures using Workbench and calculated the heat flux density intensity they endure. Through simulation experiments on the model, we successfully verified the effectiveness of the design, which improves the safety and stability of the tuyere small sleeve and reduces heat loss from the tuyere. This study provides

new ideas and directions for practical applications and new technologies for low-carbon smelting in blast furnaces.

## 2. Materials and Methods

### 2.1. Establishment of a 3D Model of the Tuyere Small Sleeve

The object of this study is the tuyere small sleeve designed for double water circulation systems, which is 630 mm long and has a diameter of 130 mm. It is welded together from four components, namely the tuyere rear-end, the tuyere front-end, the deflector, and the tuyere body, as shown in Figure 1. The tuyere small sleeve has two inlet and two outlet ports, and it is divided into two circulating cooling systems. The front-end cooling system focuses on cooling the tuyere cold head, while the rear-end cooling system cools the tuyere small sleeve body to improve its durability and safety. The deflector of the tuyere small sleeve is made of cast iron, as it offers cost-saving advantages. The remaining parts of the tuyere are constructed with copper material.

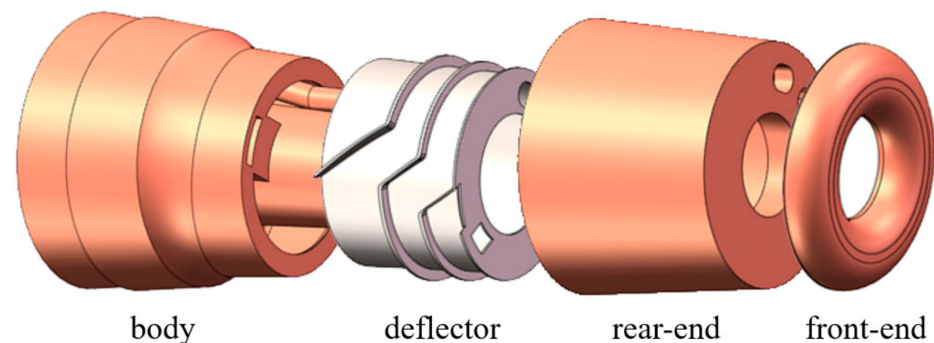


**Figure 1.** Explosion diagram of the tuyere small sleeve.

In order to investigate how to improve the wear resistance and anti-melting capacity of the tuyere small sleeve, this study used the 3D modeling software Solidworks to create a model. Subsequently, improvements were made to the structure of the wear-resistant layer, which now encompasses the front-end surface of the tuyere small sleeve. To simplify the complex heat transfer and thermal deformation behavior of the tuyere small sleeve in the blast furnace, the following simplifications and assumptions were introduced in the model [21]:

- (1) The steady-state heat conduction is adopted in the heat transfer process of the tuyere small sleeve.
- (2) There is no gap between the working surface of the tuyere and the wear-resistant coating, which is conducive to focusing on the structural changes.
- (3) It is assumed that the physical properties of the materials are fixed, and the thermal conductivity of the materials is constant in the  $x$ ,  $y$ , and  $z$  directions. The physical property parameters used in this paper are shown in Table 1, and the physical property parameters of the coating are selected from common surfacing wear-resistant materials in the literature [17,22].

**Table 1.** Physical properties of materials.

Location	Material	Density ( $\text{kg}\cdot\text{m}^{-3}$ )	Thermal Conductivity ( $\text{W}\cdot\text{m}^{-1}\cdot\text{K}^{-1}$ )	Heat Capacity ( $\text{J}\cdot\text{kg}^{-1}\cdot\text{K}^{-1}$ )
the tuyere front-end	Copper	8920	338	381
the deflector	Steel	8030	16.27	502
the tuyere body	Copper	8880	178	381
Wear-resistant layer	Nickel-based	8400	25	440
cooling medium	Water	998.2	0.6	4182

## 2.2. Establishment of a 3D Model of the Tuyere Small Sleeve

The environment of the tuyere in the blast furnace is very complex, including various parameters and variables. In order to facilitate the discussion of different positions, this study uses the designated codes in Figure 2 to represent different parts of the tuyere. In Figure 2, we can see that the front face E of the tuyere is covered with a wear-resistant layer, which is about 40 mm in length.

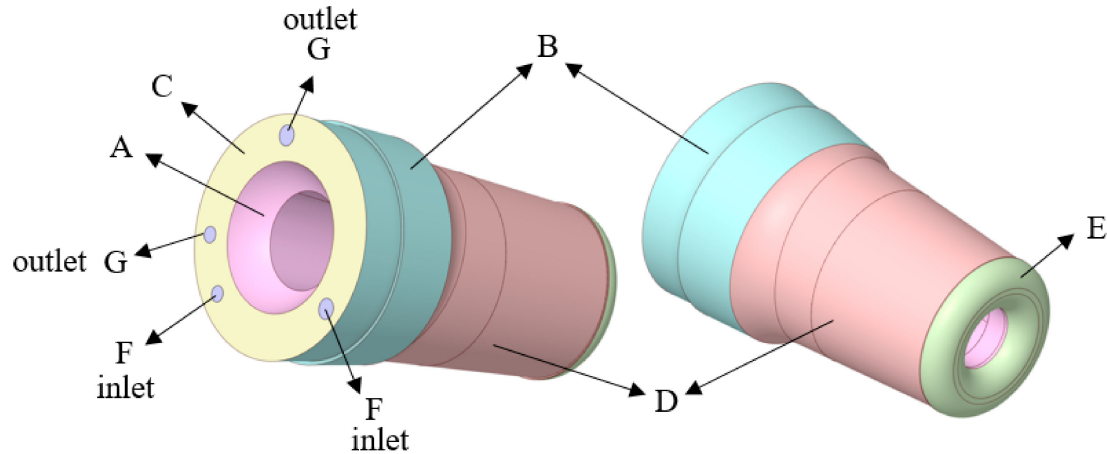


**Figure 2.** Boundary condition setting surface.

The boundary conditions for different parts of the tuyere are described in detail in Figure 2. The surface of part A of the tuyere is subjected to forced convection heat transfer from the high-temperature gas flow, and the surface heat flux at A is described as follows in the calculation:

$$q_{airflow} = h_{airflow}(T_{airflow} - T_{inner-wall}) \quad (1)$$

In the equation,  $T_{airflow}$  is the temperature of blast furnace gas inside the tuyere at 1573 K;  $T_{inner-wall}$  is the surface temperature of surface A of the tuyere in K; and  $h_{airflow}$  is the convective heat transfer coefficient of blast furnace gas, which is provided by the blast furnace factory and is 160 W/(m<sup>2</sup>·K) [23–27]. For tuyere B, because its surface is matched with the inner sleeve of the tuyere, it is simplified as an adiabatic surface in the heat transfer model. The surface of tuyere C is in contact with the environment and is simplified as convective heat transfer with the atmospheric environment. Its calculated heat flux  $q_{back-end}$  is described as:

$$q_{back-end} = h_{outside}(T_{outside} - T_{back-end}) \quad (2)$$

$T_{outside}$  is the external temperature of the rear end of the tuyere at 353 K;  $T_{back-end}$  is the temperature of the hot surface of the rear end of the tuyere, K;  $h_{outside}$  is the heat transfer coefficient of the rear end wall of the tuyere at 65 W/(m<sup>2</sup>·K). For tuyere D, its surface is subject to radiation heat transfer inside the furnace, and its heat flux calculation formula  $q_{outer-wall}$  is described as:

$$q_{outer-wall} = \varepsilon_{Cu}\sigma(T_q^4 - T_{outer-wall}^4) \quad (3)$$

$T_q$  is the temperature of the high-temperature fluid on the outer surface of the tuyere, which is 1273 K;  $T_{outer-wall}$  is the temperature of the hot surface of the tuyere at surface D, K;  $\varepsilon_{Cu}$  is the blackness coefficient of copper, 0.8;  $\sigma$  is the Boltzmann constant. For tuyere E, its surface not only undergoes forced convection heat transfer from the high-temperature

gas flow but also radiative heat transfer from high-temperature slag and iron, so a mixed consideration of heat transfer and radiation is required for the calculation of heat flux  $q_{mix}$ :

$$q_{mix} = h_{mix}(T_{bf_1} - T_{front-end}) + \varepsilon_{coating}\sigma(T_{bf_2}^4 - T_{front-end}^4) \quad (4)$$

$T_{bf_1}$  represents the temperature of intense combustion due to chemical reactions outside the wind port, which is 2273 K;  $T_{front-end}$  is the temperature of the hot surface E of the tuyere surface, K;  $T_{bf_2}$  represents the temperature of the high-temperature fluid outside the wind port, which is 2273 K;  $\varepsilon_{coating}$  is the blackness coefficient of the coating, 0.65. F represents the inlet of the tuyere, the inlet velocity is calculated based on the flow rate and the pipe diameter using a velocity inlet, the water flow rate is 33 t/h, and the water temperature is 308 K; G represents the outlet of the wind port, which uses the pressure outlet.

The heat exchange between the fluid and solid regions requires considering the influence of convective phenomena, as convection and fluid flow are generally coupled. The heat exchange heat flux  $q_w$  is described by:

$$q_w = \overline{h_w}\Delta T \quad (5)$$

$\overline{h_w}$  is the average convective heat transfer coefficient in the fluid region;  $\Delta T$  represents the temperature difference between the fluid and the inner wall of the tuyere.

The fluid region is solved using the commercially available computational fluid dynamics (CFD) software Fluent. Based on the Navier–Stokes equations, this study discretizes the three-dimensional steady-state incompressible control equations of mass conservation, momentum conservation, and energy conservation using the finite volume method.  $\rho$  and  $\mu$  represent the density and viscosity of water [28].

$$\rho \nabla \cdot (\vec{V}) = 0 \quad (6)$$

$$\rho(\vec{V} \cdot \nabla)\vec{V} = -\nabla P + \mu \nabla^2 \vec{V} \quad (7)$$

$$\nabla(\rho C_p \vec{V} T) = \nabla \cdot k \nabla T \quad (8)$$

The solution of the stress field in the tuyere is coupled with the temperature field. Since the effect of thermal stress on the temperature field is small, the model is simplified as a one-way coupling between the temperature field and the stress field. According to the theory of thermal elasticity, when a material is heated, its volume will expand and stress will be generated. The thermal deformation behavior of the tuyere can be described as follows [29]:

$$\begin{cases} \varepsilon_x = \frac{1}{E}[\sigma_x - \mu(\sigma_y + \sigma_z)] + \alpha(T - T_0), \gamma_{yz} = \frac{1}{G}\tau_{yz} \\ \varepsilon_y = \frac{1}{E}[\sigma_y - \mu(\sigma_x + \sigma_z)] + \alpha(T - T_0), \gamma_{zx} = \frac{1}{G}\tau_{zx} \\ \varepsilon_z = \frac{1}{E}[\sigma_z - \mu(\sigma_x + \sigma_y)] + \alpha(T - T_0), \gamma_{xy} = \frac{1}{G}\tau_{xy} \end{cases} \quad (9)$$

$T_0$  is the initial temperature, K;  $\varepsilon_i$  ( $i = x, y, z$ ) is the thermal strain component;  $\alpha$  is the coefficient of thermal expansion;  $G$  is the elastic modulus of the material.

### 2.3. Mesh Processing

To simulate the heat transfer of the tuyere small sleeve in a blast furnace under high-temperature conditions, Ansys Mesh software was used for model meshing. Due to the complex structure of the tuyere small sleeve, a tetrahedral-hexahedral hybrid meshing method was used to ensure the accuracy of the simulation results. The k-epsilon model was used in the fluid region to control the thickness of the first boundary layer and to achieve a target  $y^+$  value of around 30–60. Based on the calculated thickness of the first boundary layer, the size of the mesh nodes in the coupling area was determined. For the volume mesh, the mesh growth was set to start from the coupling surface until the maximum value was reached. The same mesh size control method was used for different simulation schemes,

with a mesh node count of about 5 million. Through the meshing method described above, the heat transfer and convection phenomena of the tuyere small sleeve under high-temperature conditions can be accurately described. During the simulation, we focused on the influence of each boundary condition on the simulation results and took corresponding control measures to ensure the reliability and accuracy of the simulation results.

#### 2.4. Structural Optimization Simulation Scheme

This paper proposes an annular tuyere protection layer structure for the front end of the tuyere small sleeve, which is covered with a wear-resistant layer. The structure is designed to improve the area with the highest thermal load at the front end. The design is to expose the copper surface underneath the wear-resistant layer of the tuyere, as shown in the three-dimensional model in Figure 3. As shown in the three-dimensional model in Figure 3. To determine the optimal long-life tuyere structure, numerical simulation was used to optimize the tuyere small sleeve structure and investigate the impact of different protective layer structures on tuyere heat transfer. All simulation conditions involved in this study are presented in Table 2.

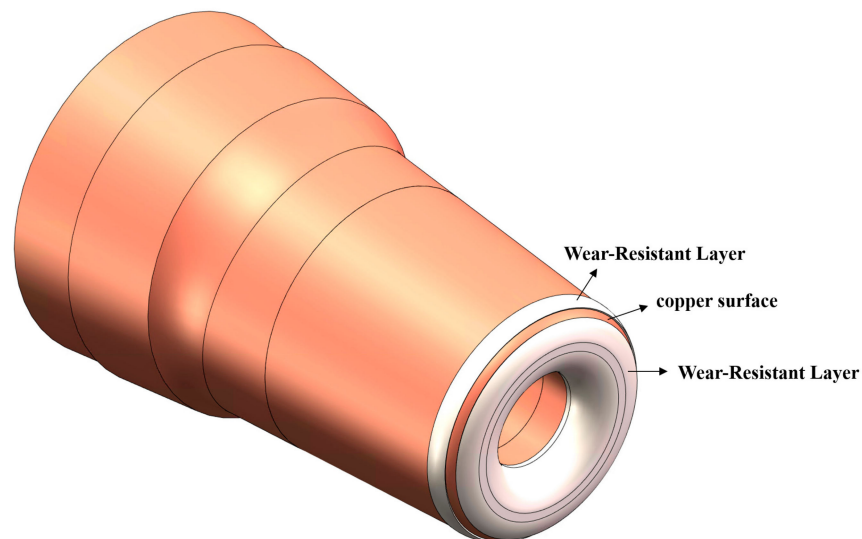


**Figure 3.** Three-dimensional model and cross-sectional view of annular wear-resistant layer.

**Table 2.** Simulation schemes.

Programme	Layer Width	Layer Thickness	Layer Thermal Conductivity	Water Flow Rate	Ambient Temperature
Case1	Uncoated	-	-	*	*
Case2	5 mm	*	*	*	*
Case3 (*)	10 mm	2	25	33	2273
Case4	15 mm	*	*	*	*
Case5	20 mm	*	*	*	*
Case6	Full coating	*	*	*	*
Case7	*	*	*	25	*
Case8	*	*	*	30	*
Case9	*	*	*	35	*
Case10	*	*	*	*	2073
Case11	*	*	*	*	2473
Case12	*	1	*	*	*
Case13	*	3	*	*	*
Case14	*	*	10	*	*
Case15	*	*	50	*	*

\* represents the same parameter settings as case 3.

### 3. Results and Discussion

#### 3.1. Investigation of the Influence of Annular Wear-Resistant Layer Opening Width

This section studies the impact of different wear-resistant coatings on the tuyere, including no coating, full coverage of the wear-resistant coating, and wear-resistant coatings with annular opening widths of 5, 10, 15, and 20 mm. As shown in Figure 4a–f by analyzing the temperature distribution of different tuyere structures, we found that the front end of the tuyere is the area where heat is concentrated, while the high-temperature region of the tuyere with the annular wear-resistant layer is concentrated on the edge of the annular opening, indicating that the edge of the annular opening may be the vulnerable part of the coating.

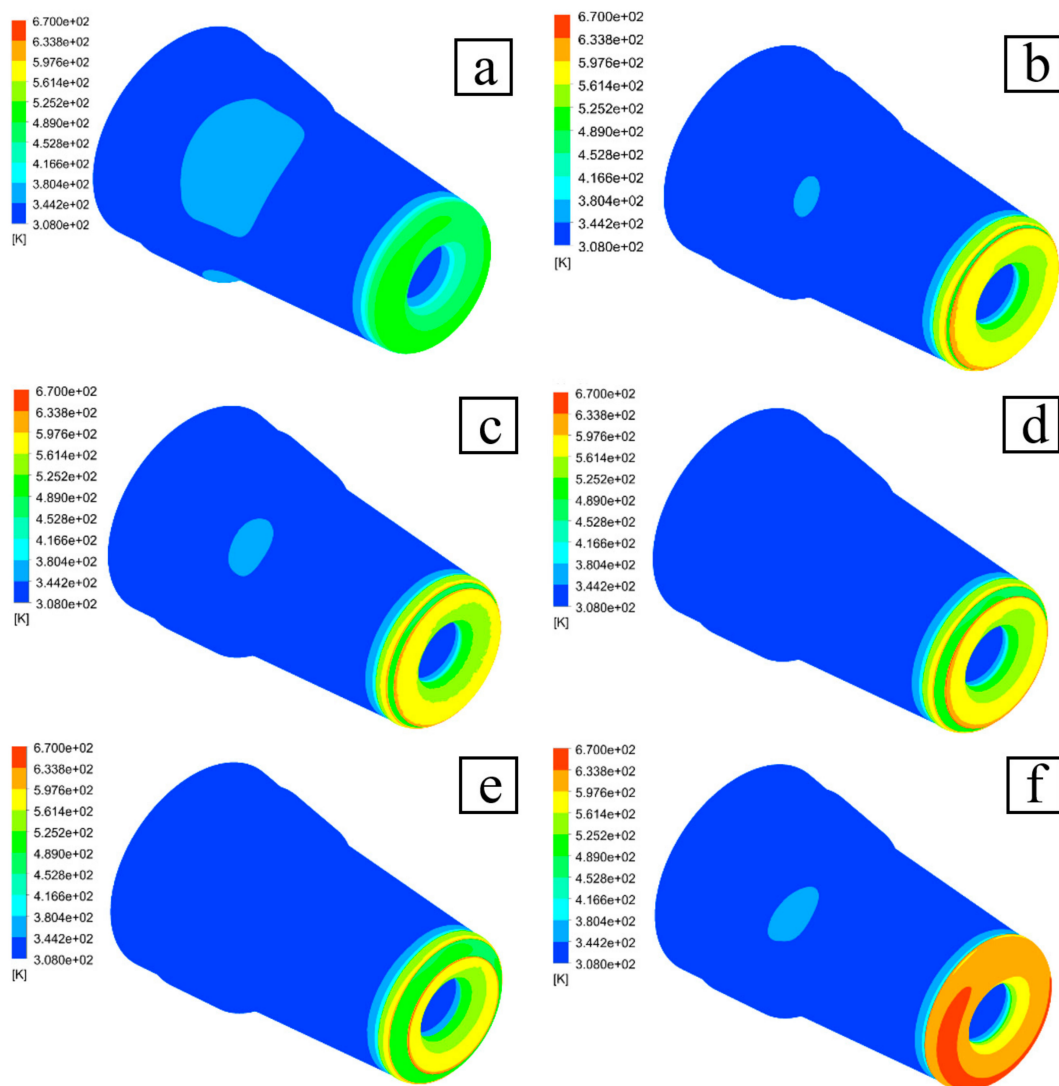


**Figure 4.** Temperature field contour maps of tuyere small sleeves with different annular wear-resistant layer opening widths: (a) Uncoated; (b) 5 mm width; (c) 10 mm width; (d) 15 mm width opening; (e) 20 mm width; (f) full coating.

To further investigate the effects of tuyere with different widths of wear-resistant layers, we calculated the highest and average temperatures of the copper substrate and the wear-resistant layer. The results are shown in Figure 5, where 0 mm width represents the temperature of the tuyere with full coverage of the wear-resistant layer, and the dotted

line represents the highest and average temperatures of the copper substrate for tuyeres without wear-resistant layers.

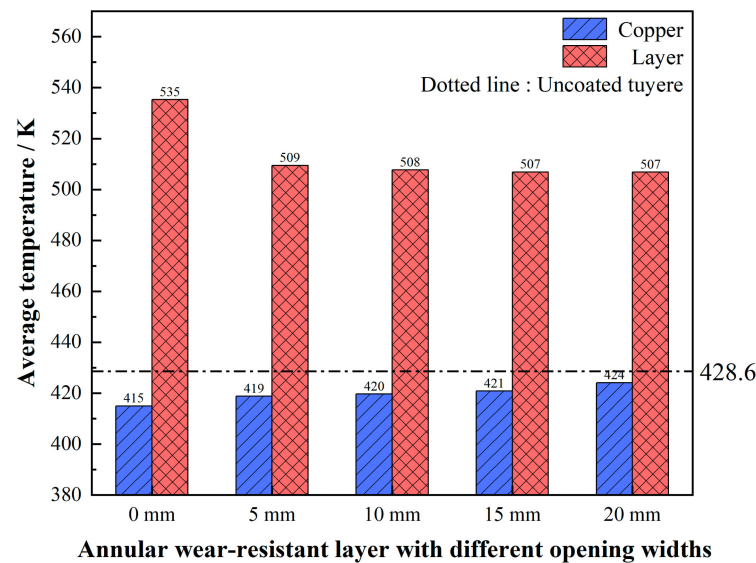


**Figure 5.** Average temperature changes of annular wear-resistant layer with different opening widths.

Based on the results presented in Figures 5 and 6, it can be observed that the average temperature of the copper matrix increases with an increase in the opening width of the annular wear-resistant layer, and similarly, the average temperature of the wear-resistant layer also increases with an increase in the opening width of the annular wear-resistant layer. The limited variation in average temperature among the coatings can be attributed to two main factors. Firstly, the negligible change in the area of the wear-resistant coating, despite the specified 5–20 mm width referring to the exposed copper surface. In reality, the variations in coating area are minimal, with proportions of 95.5%, 88.6%, 81.3%, and 70.0% for the 5 mm, 10 mm, 15 mm, and 20 mm widths, respectively. Secondly, the significant disparity in thermal conductivity between the wear-resistant layer and copper. The lower thermal conductivity of the wear-resistant layer contributes to the less pronounced temperature variations on average.

Compared to the blast furnace tuyere with a full-covered wear-resistant layer, tuyeres with different opening widths of the wear-resistant layer exhibit a significant decrease in temperature, especially for the tuyere with a 5 mm opening width of the wear-resistant layer, where the average temperature of the wear-resistant layer decreased from 535.3 K to 509.4 K, resulting in a temperature reduction of 25.9 K or 4.8%. This suggests that the wear-resistant layer has a good thermal insulation effect on the tuyere front. Although the annular wear-resistant layer tuyere slightly increases the temperature of the copper matrix at the front end, it exposes more copper surface for heat dissipation, which is beneficial for the heat dissipation of the wear-resistant layer material, and consequently, there is a significant improvement in the average temperature of the coating.

To further investigate the variation of the temperature inside the tuyere small sleeve, this study extracted temperature data from the straight line  $\alpha\beta$  on the tuyere profile and analyzed it in Figure 7a. As shown in Figure 7b, the temperature of the front end of the tuyere without coating has a greater variation and a steeper slope. The slope of the temperature variation of the front end of the annular wear-resistant layer tuyere with different opening widths is similar to that of the fully covered wear-resistant layer tuyere, indicating that the temperature variation inside the annular wear-resistant layer is similar to that of the fully covered wear-resistant layer tuyere, both of which have a good heat insulation protection effect. At the same time, the surface temperature of the wear-resistant

layer of the fully covered wear-resistant layer tuyere is higher, while the surface temperature of the wear-resistant layer of the annular wear-resistant layer tuyere is between the two.

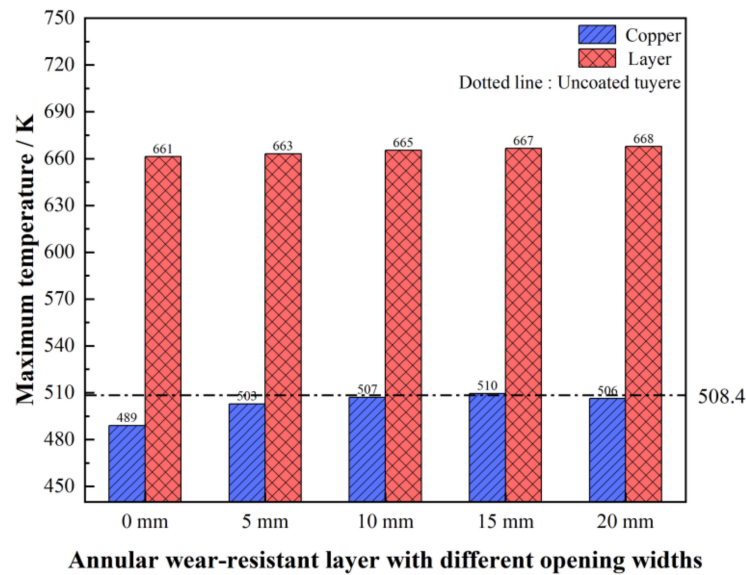


Figure 6. Maximum temperature variation of annular wear-resistant layer with different opening widths.

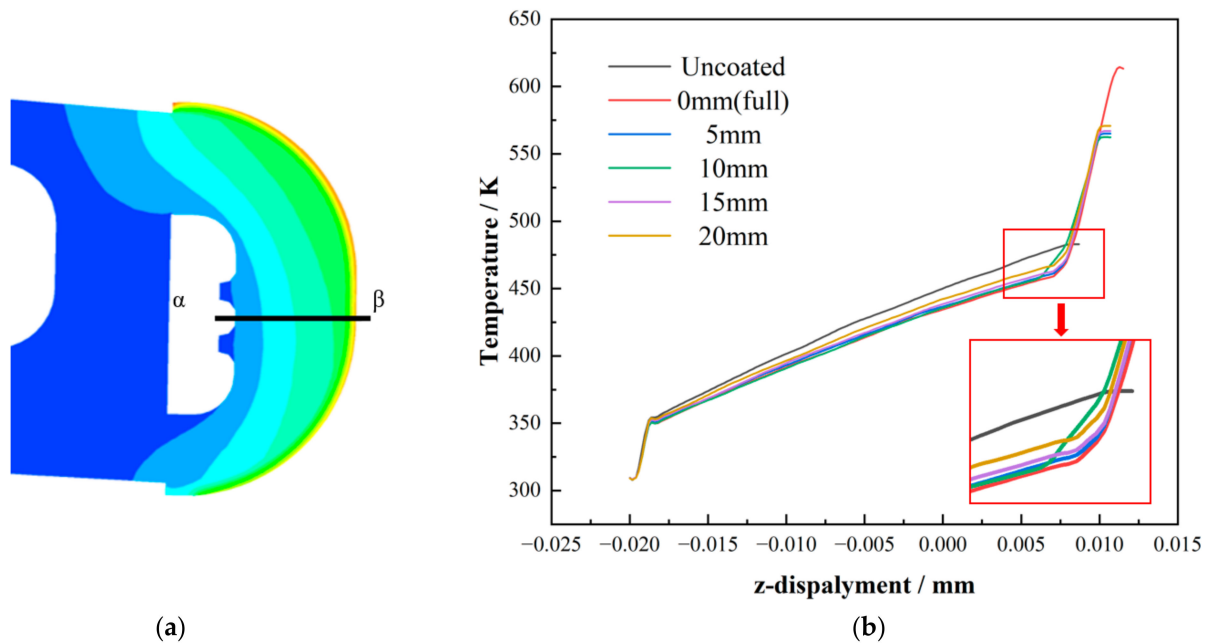
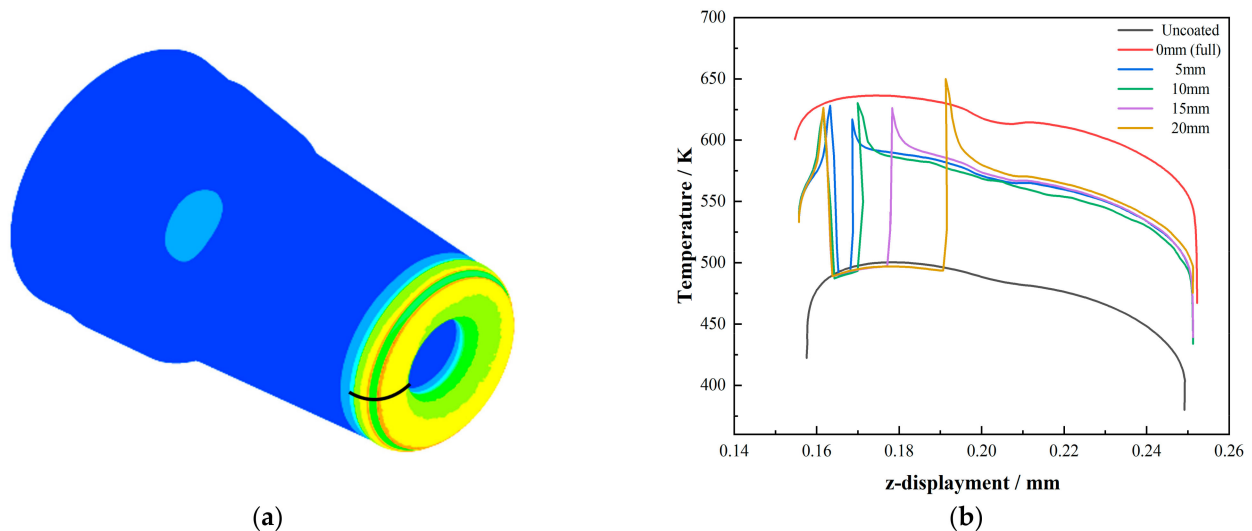


Figure 7. (a) Tuiere profile (b) Tuiere section temperature variation.

To further study the variation of the surface temperature of the blast furnace tuyere, this study selected the temperature data on the surface of the tuyere in Figure 8 for analysis. As shown in Figure 8b, the surface temperature of the wear-resistant coating of the fully covered tuyere is much higher than that of the uncoated tuyere. The surface temperature of the wear-resistant coating of the annular wear-resistant layer tuyere is between the two, and the temperature of the exposed copper of the annular wear-resistant layer tuyere with a large opening width is comparable to the surface temperature of the uncoated tuyere. Therefore, the results in Figure 8 indicate that the annular wear-resistant layer structure has an important effect on the surface temperature of the tuyere, and the annular wear-resistant

layer tuyere with a large opening width can effectively reduce the surface temperature, which also indicates that the wear-resistant layer opening is indeed beneficial for the heat dissipation of the tuyere small sleeve. The reduction in the average temperature of the coating is beneficial for reducing thermal stress and prolonging the service life of the coating, thereby extending the service life of the tuyere small sleeve.



**Figure 8.** (a) Tuyere surface monitoring location (b) Temperature variation of tuyere surface.

By calculating the inlet and outlet water temperatures for each model under the simulated conditions, the heat flux density for different structures can be obtained, as shown in Table 3. From Table 3, it can be seen that the heat flux density of the uncoated tuyere small sleeve is the highest at  $276.99 \text{ kW/m}^2$ , while the fully coated tuyere small sleeve has the lowest heat flux density at  $208.96 \text{ kW/m}^2$ . The heat flux density of the annular wear-resistant layer of tuyere small sleeve is between the two and increases with the width of the annular opening. Combining with the simulation results of the temperature field in the previous section, the optimal annular wear-resistant layer of tuyere small sleeve structure is 5–10 mm in width, which can not only reduce the temperature on the surface of the coating but also retain the heat insulation and wear resistance properties of the coating. Compared with the uncoated tuyere small sleeve, the heat flux density is reduced by 16.7%, which can save 130–140 kg of coke per tuyere small sleeve per day according to calculations. This is equivalent to a  $4000 \text{ m}^3$  blast furnace with 40 tuyeres and a utilization coefficient of 2.0, which can reduce the coke ratio by 0.78 kg/t (ton of iron). This is a new train of thought for low-carbon blast furnace smelting technology.

**Table 3.** Temperature difference and heat flux density intensity of tuyere in blast furnace.

Different Case	Back-End Water Temperature Difference (K)	Front-End Water Temperature Difference (K)	Heat Flux Density ( $\text{kW/m}^2$ )
full coating	2.41	3.15	208.96
5 mm	2.79	3.22	225.87
10 mm	2.88	3.26	230.76
15 mm	2.98	3.26	236.02
20 mm	3.02	3.48	244.29
Uncoated	3.77	3.60	276.99

### 3.2. Study on the Influence of Different Parameters on the New Type of Tuyere

To ensure stable operation of the new blast furnace tuyere, simulation under different parameter conditions is necessary. In this study, the maximum and average temperatures on the front face of the tuyere small sleeve with a 10 mm width of the annular wear-resistant layer were calculated, as well as the maximum and average temperatures of the wear-resistant layer, under different water-flow rates and blast furnace ambient temperatures, with wear-resistant layer thicknesses of 1 mm, 2 mm, and 3 mm and thermal conductivity values of 10, 25, and 50 W/(m·K).

The results of Figure 9 indicate that, for the copper substrate, the temperature in the high-temperature zone of the blast furnace has the greatest impact on its temperature, followed by the coating thickness, water flow rate, and coating thermal conductivity. For the coating, the thermal conductivity of the coating has the greatest influence on its temperature, followed by the blast furnace ambient temperature, coating thickness, and water flow rate. When the temperature of the tuyere copper substrate is maintained above 473 K for a long time, the physical properties of the tuyere sleeve will decrease significantly due to the growth of internal copper grains [1,16,30]. Therefore, in actual production, it is necessary to maintain a high water speed and control the blast furnace's ambient temperature within a safe range. Figure 9 shows that when the blast furnace ambient temperature is below 2273 K and the water flow rate is above 30 t/h, the tuyere sleeve with a ring-shaped wear-resistant layer is in a safe state.

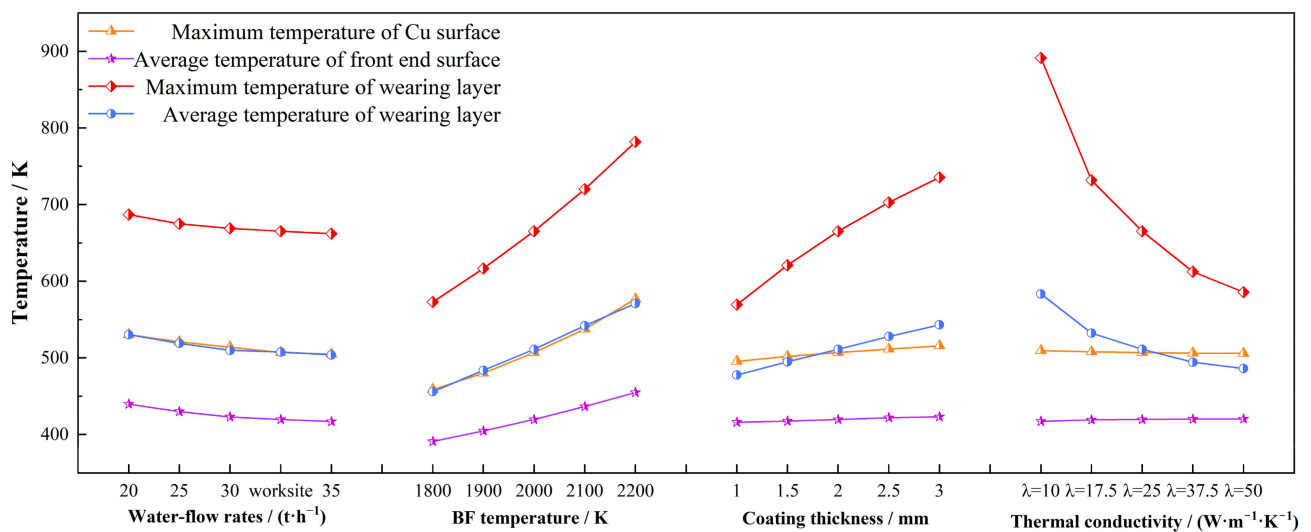
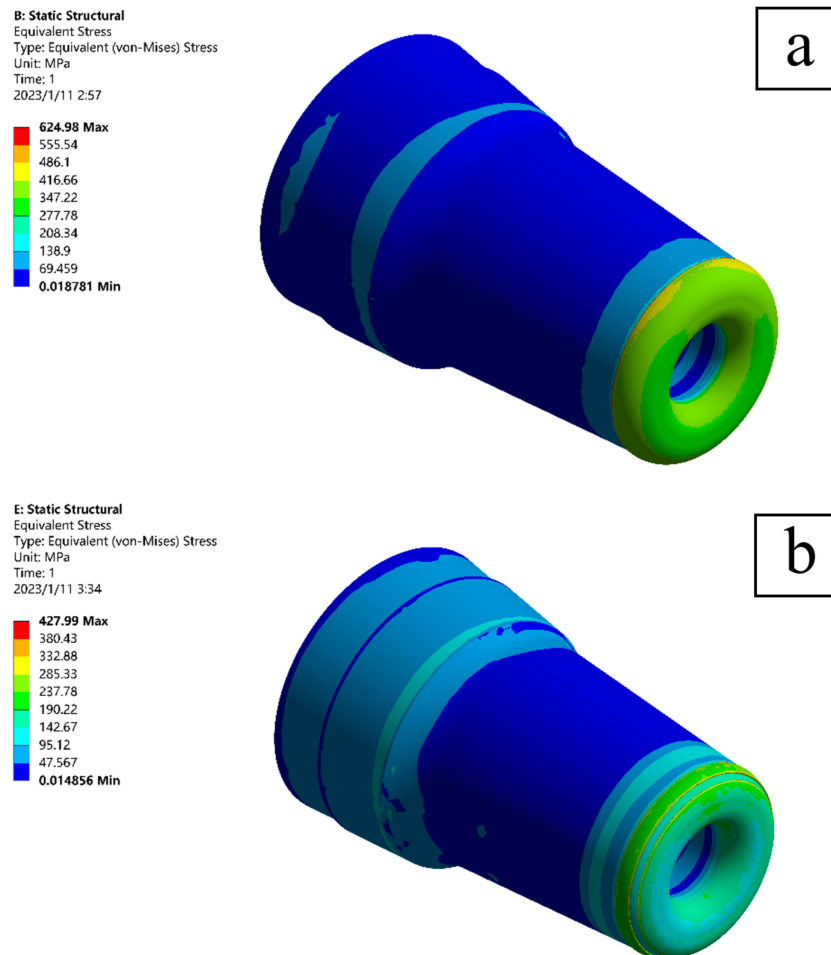


Figure 9. Influence of different conditions on tuyere temperature.

### 3.3. Simulation of Stress Field in Annular Wear-Resistant Layer Structure Tuyere

This section investigates the thermal stress problem of the tuyere front wear layer. In order to explore the stress distribution of different tuyere structures, numerical simulations of the stress field were conducted for both full-coated wear layer tuyeres and 10 mm-width annular wear layer tuyeres under the same conditions, and the results were compared. Figure 10a shows that the surface stress of the full-coated wear layer tuyere is mostly between 350–400 MPa, with the highest surface stress being 624.98 MPa. Figure 10b shows that the surface stress of the annular wear layer tuyere is mostly between 180–230 MPa, with the highest surface stress being 427.99 MPa, concentrated on the edges of the annular wear layer, which may cause the wear layer to peel off from the edges. However, it should be noted that the coating stress of the annular wear layer tuyere is far lower than that of the full-coated wear layer tuyere, and the highest stress of the annular wear layer tuyere is reduced by 31.5%, indicating that the design of the annular wear layer tuyere is beneficial to reducing the coating stress and extending the service life of the coating.

These results not only have reference value for the design of annular wear layer tuyeres but also have some guiding significance for the design of other types of tuyeres and similar high-temperature equipment.



**Figure 10.** (a) Stress field of the full-coverage wear-resistant layer tuyere; (b) Stress field of the annular wear-resistant layer tuyere.

#### 4. Conclusions

This paper provides a detailed comparison of the temperature field differences between tuyere small sleeves with and without coatings and those with different widths of the annular wear-resistant layer structure. Calculated the heat flow intensity of tuyere small sleeves passing through different structures. Computed the influence of different parameters on the temperature field of the new structure of the tuyere small sleeve. Finally, the stress field of the new structure tuyere small sleeve was compared with that of the fully covered coated tuyere small sleeve through simulation. Through the study in this paper, the following conclusions were drawn:

- (1) The design of an annular wear-resistant layer for the tuyere small sleeve is effective. The simulation results demonstrate that the optimal width for the annular wear-resistant layer is between 5 mm and 10 mm, which can reduce the coating temperature by 24 K. This design can reduce heat loss in the tuyere area of the blast furnace by 16.7%, providing new technological solutions for low-carbon production. The annular wear-resistant layer design for the tuyere presents a potential economic benefit by reducing the coke ratio by 0.78 kg/t (ton of iron).
- (2) The copper base of the annular wear-resistant layer tuyere small sleeve remains stable under different conditions, and the 10 mm-width annular wear-resistant layer tuyere

small sleeve is within a safe temperature range when the blast furnace environment temperature is below 2273 K.

- (3) The simulation results of the stress field indicate that the stress is concentrated at the edge of the coating for the tuyere small sleeve with the annular wear-resistant layer structure. The overall stress of the coating is lower than that of the fully covered coated tuyere small sleeve, and the maximum thermal stress is reduced by 31.5%. The design of the annular wear-resistant layer is beneficial for extending the service life of the coating, thereby extending the service life of the tuyere small sleeve.

**Author Contributions:** Conceptualization, J.Z.; methodology, Y.Z.; software, L.Z.; validation, W.Z., L.Z. and K.J.; formal analysis, W.Z.; investigation, Y.L.; resources, L.Y.; data curation, W.Z. and L.Y.; writing—original draft preparation, W.Z.; writing—review and editing, L.Z.; supervision, K.J.; project administration, J.Z. All authors have read and agreed to the published version of the manuscript.

**Funding:** This research received no external funding.

**Data Availability Statement:** Not applicable.

**Acknowledgments:** This work was financially supported by Key Laboratory of Metallurgical Industry Safety & Risk Prevention and Control, Ministry of Emergency Management.

**Conflicts of Interest:** No potential conflict of interest was reported by the authors.

## References

1. Chung, J.-K.; Hur, N.-S. Tuyere Level Coke Characteristics in Blast Furnace with Pulverized Coal Injection. *ISIJ Int.* **1997**, *37*, 119–125. [[CrossRef](#)]
2. Gao, T.L.; Jiao, K.X.; Ma, H.B.; Zhang, J.L. Analysis of tuyere failure categories in 5800 m<sup>3</sup> blast furnace. *Ironmak. Steelmak.* **2020**, *48*, 586–591. [[CrossRef](#)]
3. Gao, T.; Jiao, K.; Zhang, J.; Ma, H. Melting Erosion failure mechanism of tuyere in blast furnace. *ISIJ Int.* **2021**, *61*, 71–78. [[CrossRef](#)]
4. Farkas, O.; Móger, R. Metallographic aspects of Blast Furnace tuyere erosion processes. *Steel Res. Int.* **2013**, *84*, 1171–1178. [[CrossRef](#)]
5. Portnov, L.V.; Nikitin, L.D.; Bugaev, S.F.; Shchipitsyn, V.G. Improving the durability of blast-furnace tuyeres. *Metallurgist* **2014**, *58*, 488–491. [[CrossRef](#)]
6. You, Y.; Zheng, Z.; Wang, R.; Hu, Q.; Li, Y.; You, Z. Numerical Study on Combustion Behavior of Semi-Coke in Blast Furnace Blowpipe-Tuyere-Combustion Zone. *Metals* **2022**, *12*, 1272. [[CrossRef](#)]
7. Goloshchapov, K.V.; Kobelev, O.A.; Titlyanov, A.E.; Borisov, P.V.; Makarov, P.S.; Chicheneva, O.N. Improvement of the function of blast-furnace air tuyeres. *Metallurgist* **2022**, *66*, 215–220. [[CrossRef](#)]
8. Zainullin, L.A.; Epishin, A.Y.; Spirin, N.A. Extending the life of blast-furnace air tuyeres. *Metallurgist* **2018**, *62*, 322–325. [[CrossRef](#)]
9. Chatterjee, R.; Nag, S.; Kundu, S.; Ghosh, U.; Singh, U.; Chandra, S. Impact of flow boiling on blast furnace tuyere life: A designer's perspective. *Steel Res. Int.* **2022**, *93*, 12. [[CrossRef](#)]
10. Chatterjee, R.; Nag, S.; Kundu, S.; Chakraborty, R.; Singh, U.; Chandra, S. Erosion behavior of blast furnace tuyere. *ISIJ Int.* **2019**, *59*, 1732–1734. [[CrossRef](#)]
11. Chatterjee, R.; Nag, S.; Kundu, S.; Ghosh, U.; Padmapal; Singh, U. A journey towards improving tuyere life. *Trans. Indian Inst. Met.* **2021**, *74*, 1077–1088. [[CrossRef](#)]
12. Guo, X.P.; Han, W.Y. The numerical simulation analysis of tuyere's temperature field and stress field. *Adv. Mater. Res.* **2013**, *706*, 1701–1704. [[CrossRef](#)]
13. Radyuk, G.; Titlyanov, A.E.; Sidorova, T.Y. Effect of slurry coating on the resistance of thermal insulation insert in blast furnace air tuyere. *Metallurgist* **2020**, *63*, 1153–1159. [[CrossRef](#)]
14. Tarasov, Y.S.; Skripalenko, M.M.; Radyuk, A.G.; Titlyanov, A.E. Effect of the thermal insulation of the inner wall on the thermal condition of the air tuyeres of blast furnaces. *Metallurgist* **2018**, *61*, 745–750. [[CrossRef](#)]
15. Tarasov, Y.S.; Skripalenko, M.M.; Radyuk, A.G.; Titlyanov, A.E. Computer simulation of thermal and stress-strain state of blast furnace tuyeres. *Metallurgist* **2019**, *62*, 1083–1091. [[CrossRef](#)]
16. Zhang, J.; Wang, R.; Hu, R.; Zhang, C.; Li, G.; Zhang, Y.; Wu, W.; Lu, X. Failure mode and mechanism of a blast furnace tuyere. *Eng. Fail. Anal.* **2022**, *137*, 106294. [[CrossRef](#)]
17. Chen, Z.; Zhang, C.; Zhang, J.; Zhang, Y.; Wu, W.; Li, G.; Lu, X. Temperature field simulation of Ni60A coating with different copper content on blast furnace tuyere. *Mater. Today Commun.* **2022**, *32*, 104093. [[CrossRef](#)]
18. Li, D.; Zhang, C.; Wang, R.; Zhang, J.; Hu, R.; Zhang, Y.; Li, G.; Lu, X. Microstructure and properties evolution of Co06/Ni60A duplex coating on copper by plasma cladding. *Surf. Coat. Technol.* **2021**, *429*, 127978. [[CrossRef](#)]
19. Titov, V.N.; Ternovikh, A.I.; Baranov, P.V.; Sidorova, T.Y. Development of coatings for protection of blast furnace air tuyeres. *Metallurgist* **2021**, *65*, 439–445. [[CrossRef](#)]

20. Pathak, A.; Sivakumar, G.; Prusty, D.; Shalini, J.; Dutta, M.; Joshi, S.V. Thermal spray coatings for blast furnace tuyere application. *J. Therm. Spray Technol.* **2015**, *24*, 1429–1440. [[CrossRef](#)]
21. Liu, Q.; Cheng, S. Heat transfer and thermal deformation analyses of a copper stove used in the belly and lower shaft area of a blast furnace. *Int. J. Therm. Sci.* **2015**, *100*, 202–212. [[CrossRef](#)]
22. Shmorgun, V.G.; Bogdanov, A.I.; Taube, A.O.; Kulevich, V.P. Evaluation of heat resistance and thermal conductivity of Ni–Cr–Al system layered coatings. *Metallurgist* **2022**, *66*, 934–941. [[CrossRef](#)]
23. Titov, V.N.; Saifullaev, S.D.; Skripalenko, M.M.; Ternovykh, A.I.; Sidorov, A.A. Using DEFORM-2D software to study heat-insulation materials as protection of air tuyeres against burnout. *Metallurgist* **2020**, *64*, 388–395. [[CrossRef](#)]
24. Radyuk, A.G.; Titlyanov, A.E.; Skripalenko, M.M.; Stoishich, S.S. Modeling of the temperature field of air tuyeres in the blast furnaces with thermal insulation of the nose portion. *Metallurgist* **2018**, *62*, 310–313. [[CrossRef](#)]
25. Radyuk, A.G.; Titlyanov, A.E.; Skripalenko, M.M. Modeling of the temperature field of blast furnace tuyeres using Deform-2D software. *Metallurgist* **2017**, *60*, 1011–1015. [[CrossRef](#)]
26. Shen, Y.-S.; Liu, Z.-M.; Zhu, T.; Yan, F.-S.; Xin, H.-N.; Sun, R.-L. The new technology and the partial thermotechnical computation for air-cooled blast furnace tuyere. *Appl. Therm. Eng.* **2009**, *29*, 1232–1238. [[CrossRef](#)]
27. Wang, K.; Zhou, H.; Si, Y.; Li, S.; Ji, P.; Wu, J.; Zhang, J.; Wu, S.; Kou, M. Numerical analysis of natural gas injection in shougang jingtang blast furnace. *Metals* **2022**, *12*, 2107. [[CrossRef](#)]
28. Liu, Q.; Zhang, P.; Cheng, S.; Niu, J.; Liu, D. Heat transfer and thermo-elastic analysis of copper steel composite stove. *Int. J. Heat Mass Transf.* **2016**, *103*, 341–348. [[CrossRef](#)]
29. Wu, L.; Xu, X.; Zhou, W.; Su, Y.; Li, X. Heat transfer analysis of blast furnace stove. *Int. J. Heat Mass Transf.* **2008**, *51*, 2824–2833. [[CrossRef](#)]
30. Zasadzińska, M.; Knych, T.; Strzypek, P.; Jurkiewicz, B.; Franczak, K. Analysis of the strengthening and recrystallization of electrolytic copper (Cu-ETP) and oxygen free copper (Cu-OF). *Arch. Civ. Mech. Eng.* **2018**, *19*, 186–193. [[CrossRef](#)]

**Disclaimer/Publisher’s Note:** The statements, opinions and data contained in all publications are solely those of the individual author(s) and contributor(s) and not of MDPI and/or the editor(s). MDPI and/or the editor(s) disclaim responsibility for any injury to people or property resulting from any ideas, methods, instructions or products referred to in the content.